UNIVERSITY OF COPENHAGEN

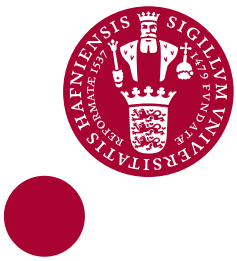

# Heavy metal exposure causes changes in the metabolic health-associated gut microbiome and metabolites

Li, Xuan Ji; Brejnrod, Asker Daniel; Ernst, Madeleine; Rykær, Martin; Herschend, Jakob; Olsen, Nanna Mee Coops; Dorrestein, Pieter C.; Rensing, Christopher; Sørensen, Søren Johannes

*Published in:*
Environment International

*DOI:*
10.1016/j.envint.2019.02.048

*Publication date:*
2019

*Document version*
Publisher's PDF, also known as Version of record

*Document license:*
CC BY-NC-ND

*Citation for published version (APA):*
Li, X. J., Brejnrod, A. D., Ernst, M., Rykær, M., Herschend, J., Olsen, N. M. C., Dorrestein, P. C., Rensing, C., & Sørensen, S. J. (2019). Heavy metal exposure causes changes in the metabolic health-associated gut microbiome and metabolites. *Environment International*, *126*, 454-467. https://doi.org/10.1016/j.envint.2019.02.048

Download date: 04. May. 2023

Environment International 126 (2019) 454–467

Contents lists available at ScienceDirect

Environment International

journal homepage: www.elsevier.com/locate/envint

# Heavy metal exposure causes changes in the metabolic health-associated gut microbiome and metabolites

Xuanji Li[a,1], Asker Daniel Brejnrod[b,1], Madeleine Ernst[c,d], Martin Rykær[e,f], Jakob Herschend[a], Nanna Mee Coops Olsen[a], Pieter C. Dorrestein[c,d,g], Christopher Rensing[h,*], Søren Johannes Sørensen[a,**]

[a] Department of Biology, University of Copenhagen, Copenhagen, Denmark
[b] Novo Nordisk Foundation Center for Basic Metabolic Research, Section of Metabolic Genetics, University of Copenhagen, Copenhagen, Denmark
[c] Collaborative Mass Spectrometry Innovation Center, Skaggs School of Pharmacy and Pharmaceutical Sciences, University of California, San Diego, United States of America
[d] Skaggs School of Pharmacy and Pharmaceutical Sciences, University of California, San Diego, United States of America
[e] Novo Nordisk Foundation Center for Protein Research, Copenhagen University, Copenhagen, Denmark
[f] Department of Biotechnology and Biomedicine, Technical University of Denmark, Kgs. Lyngby, Denmark
[g] Center for Microbiome Innovation, University of California, San Diego, United States of America
[h] Fujian Provincial Key Laboratory of Soil Environmental Health and Regulation, College of Resources and Environment, Fujian Agriculture and Forestry University, Fuzhou, China

ARTICLE INFO

Handling Editor: Yong-Guan Zhu

*Keywords:*
Arsenic
Cadmium
T2DM
16S rRNA microbiome
LC-MS/MS metabolomics

ABSTRACT

*Background:* Exposure to arsenic and cadmium is common. Epidemiological and animal studies have suggested that exposure to these two heavy metals can cause metabolic health problems, including type 2 diabetes (T2DM). It has been hypothesized that T2DM could be mediated through the gut microbiome and the metabolites it produces. Although many studies have investigated the association between the gut microbiome and T2DM, few have focused on the connection to arsenic and cadmium.

*Results:* We applied 16S rRNA gene amplicon sequencing and untargeted LC-MS/MS metabolomics to examine the changes in the gut microbiome and metabolite profiles of exposed mice to relevant levels of cadmium and arsenic in the drinking water over two weeks. Cadmium chloride (Cd) exposure significantly changed the mice gut microbiome and resulted in a significantly lower microbial diversity whereas sodium arsenite (As) caused a non-significant decrease in microbial diversity. For Cd and As treatment respectively, we identified 5 and 2 phyla with significant changes and 42 and 24 genera. Bacterial genera that were observed to decline upon both treatments, included several butyrate-producers. Both As and Cd treatment perturbed the metabolome significantly, with 50 ppm Cd compound exposure having the greatest effect when compared to 50 ppm As compound exposure. Two unidentified features were differentially abundant in the As group, while 33 features changed in the Cd group. Differential abundance analysis of all bile acid associated molecular components showed differences under both treatments. Finally, integrative network analysis via bipartite correlation networks suggested that several genera, including the metabolically important *Blautia*, *Eisenbergiella*, *Clostridium_XlVa*, etc. declined in numbers of metabolite interactions.

*Conclusions:* These results demonstrated that As and Cd exposure caused significant changes to the gut microbiome and metabolome by affecting bile acids, amino acids and taxa associated with metabolic health.

## 1. Introduction

Diabetes mellitus is a worldwide metabolic syndrome, which is characterized by fasting hyperglycemia, insulin secretory dysfunction or insulin resistance (Kim et al., 2001). According to a report from the International Diabetes Federation, the diabetic population now stands at about 382 million (8.3% of adults) globally and is estimated to rise to 592 million people (10% of adults) by 2035 (Guariguata et al., 2014).

* Correspondence to: C. Rensing, No.15 Shangxiadian Road, Cangshan District, Fuzhou, Fujian, China.
** Correspondence to: S.J. Sørensen, Universitetsparken 15, bldg. 1, DK2100 Copenhagen, Denmark.
*E-mail addresses:* rensing@fafu.edu.cn (C. Rensing), sjs@bio.ku.dk (S.J. Sørensen).
[1] Xuanji Li and Asker Daniel Brejnrod have contributed equally.

https://doi.org/10.1016/j.envint.2019.02.048
Received 10 October 2018; Received in revised form 18 February 2019; Accepted 19 February 2019
0160-4120/ © 2019 Published by Elsevier Ltd. This is an open access article under the CC BY-NC-ND license (http://creativecommons.org/licenses/BY-NC-ND/4.0/).

Among the different types of diabetes, type 2 diabetes (T2DM) is the most prevalent, accounting for 90–95% of all cases (Wild et al., 2004). Traditional T2DM risk factors include age, obesity, lifestyle and, in some rare instances, genetic predisposition (Jääskeläinen et al., 2013). However, these factors seem insufficient to explain the mounting worldwide T2DM epidemic. Some epidemiological studies have shown that environmental chemicals may play an etiological role in the progression of T2DM (Jeon et al., 2015). As exposure has been linked to the impairment of glucose metabolism (Jeon et al., 2015). Hundreds of millions of people around the world live in regions where natural As concentration in drinking water far exceeds the safety standard of 10 μg/L accepted by the World Health Organization and the U.S. Environmental Protection Agency (EPA) (Chen et al., 2009; Hughes et al., 2011). The occurrence of As contamination in soil and ground water caused by human activities is also very common (Jeon et al., 2015). Cadmium (Cd) is also known as a highly toxic heavy metal that poses increasing risk to populations in many parts of the world (Diawara et al., 2006; Edwards and Prozialeck, 2009). Studies suggest that low but chronic levels of Cd exposure can impair the function of insulin-producing β-cells and may be associated with T2DM (El Muayed et al., 2012). Cigarette smoke and diet are among the main routes of Cd for nonoccupational Cd exposure (Madeddu et al., 2009; El Muayed et al., 2012). Despite high toxicity and easy accessibility, so far, only a handful of studies mainly from epidemic and animal physiological research provide proofs for the adverse effects of the two metals on health.

Accumulating evidence from animal and human studies suggest that alteration of the gut microbiome through dietary manipulation and the presence of environmental pollutants may disturb physiological and metabolic homeostasis, contributing in part to the development of various diseases (Everard and Cani, 2013; He et al., 2015; Larsen et al., 2010). As and Cd exposure have been reported to result in changes of gut microbiota and metabolic profiles in some exploratory mice studies (Liu et al., 2014; Lu et al., 2014), however T2DM was not the study target. T2DM has also been reported to be closely associated with the gut microbiome (He et al., 2015; Larsen et al., 2010; Qin et al., 2012). For example, gram-negative bacteria in the gut have received much attention for their role in the development of diabetes (Amar et al., 2011; Cani et al., 2007). A major compound in the outer membrane of gram-negative bacteria are lipopolysaccharides (LPS), which are potent stimulators of the immune system causing inflammations and endotoxemia (Nielsen et al., 2003). Consequently, the continuous LPS production within the gut might trigger an inflammatory response and further promote the development of diabetes. Furthermore, some specific groups of gram-negative bacteria have received more attention recently, as they have been linked to gut microbiome dysbiosis. *Akkermansia muciniphila*, an important intestinal mucus-degrading gram-negative bacterium that accounts for densities of up to 3% of the total number of bacteria in adult feces, was linked to diabetes and obesity (Everard et al., 2013; Plovier et al., 2017). In this study, we specifically focused on gram-negative bacteria by treatment with vancomycin to enrich for this type of bacteria in a murine model. This treatment is known to induce a dysbiotic state in both humans (Vrieze et al., 2014; Zarrinpar et al., 2018) and mice (Hansen et al., 2012). The result of this treatment impacts a wide range of metabolic outputs from the microbiome such as bile acids and short chain fatty acids. To observe the effect of the intervention, control mice were also treated with vancomycin. We used a combination of 16S rRNA gene sequencing and liquid chromatography coupled to tandem mass spectrometry (LC-MS/MS) based metabolomics to analyze the alterations in the murine gut microbiome and its metabolic profile induced by exposure to As and Cd.

## 2. Material and methods

### 2.1. Chemicals, animals, and experimental protocol

Five-week-old C57BL/6 mice were purchased from the China National Laboratory Animal Resource Center. All the operations in the animal experiment were followed by the 3R principle (Russell and Burch, 1959). A total of 48 mice (body weight = 20 ± 3 g) were housed in static microisolator cages (4 mice/cage) under environmental conditions of 22 °C, 40–70% humidity, and a 12:12 h light:dark cycle. Water and food was available ad libitum during the whole experiment. Mice were treated with 500 mg/L vancomycin in the drinking water for one week after one-week initial adaption to cage-food and laboratory conditions. Afterwards, the mice were randomly divided into 3 experimental groups containing 16 animals each (4 mice/cage). One group, serving as a control drank water free of contaminants, and the other two groups were separately treated with 50 ppm cadmium chloride (Cd) (equals to 0.273 mmol/L $Cd^{2+}$) or 50 ppm sodium arsenite (As) (equals to 0.385 mmol/L $As^{3+}$) supplied in the drinking water for 2 weeks. Mice were assessed every day for signs of diarrhea, dehydration, mortality and deteriorating body conditions. Body weight, food and water intake were assessed twice per week during the Cd/As treatment. All mice were sacrificed after anesthetization with ether on the last day of the treatment. Colon and caecum content were collected and stored at −80 °C before use. During the experiment, three animals in the As group died from fight trauma.

### 2.2. 16S rRNA gene sequencing and analysis

Genomic DNA was extracted from colonic content with the QIAamp PowerFecal DNA Kit (Qiagen, Hilden, Germany) according to the manufacturer's instruction. All operations were performed under aseptic conditions. The NanoDrop spectrophotometer (Thermo Scientific NanoDrop Products) was used to check DNA concentration and a 1% agarose gel was used to test DNA quality. The 16S rRNA gene hypervariable V3-V4 region was amplified with 1 μL template DNA (10–50 ng/μL), using 12.5 μL KAPA HiFi HotStart Ready Mix (Anachem, Dublin, Ireland), 0.25 μL 25 μM of each primer were PCR amplified using 25 cycles with the primers Bakt_341F (CCTACGGGNGGCWGCAG) and Bakt_805R (GACTACHVGGGTATCTAATCC) (Klindworth et al., 2013) in a 25 μL PCR reaction volume. The first PCR program included 3 min at 95 °C, 25 cycles of 30 s at 95 °C, 30 s at 55 °C, and 72 °C for 30 s, and then 5 min at 72 °C. In the second PCR, the sequencing primers and adaptors were attached to the amplicon library following the first PCR conditions with only 8 cycles. The size of the PCR product was evaluated using gel electrophoresis. The amplicon products were purified by use of Agencourt AMPure XP Beads (Beckman Coulter Genomics, MA, USA) and were quantified by densitometry using Quantity one software (Bio-Rad, Hercules, CA, USA), then pooled in equimolar concentrations. The purification of DNA library was done by gel extraction with the Qiagen gel extraction kit (Qiagen, Hilden, Germany). The concentration and length distribution of DNA library was checked by Qubit Fluorometer (Invitrogen, Carlsbad, CA, USA) and Qseq100 (BiOptic Inc., Taiwan, China). Sequencing of V4 region of bacterial 16S rRNA genes was performed with Miseq PE300 platform as previously described (Lu et al., 2015). The obtained paired-end raw data was assembled by Flash (Magoč and Salzberg, 2011). Quality filtered, Length trimming, Homopolymer truncation were processed by mothur (Schloss et al., 2009). OTU clustering and Taxonomy classification was carried out by UPARSE, v9.0.2132 (Edgar, 2013), sorting 1,937,439 reads into 662 OTUs at 97% sequence homology. The open source statistical program “R” was used for data treatment and analysis (R Development Core Team, 2011), predominantly the R-package “phyloseq” (McMurdie and Holmes, 2013). Alpha diversity between the groups was tested by analysis of variance, using the R function “aov”. UniFrac distance (Lozupone and Knight, 2005), ordinated by principal

coordinates analysis (PCoA, R function "ordination", R-package "phyloseq"), was examined by permutational multivariate analysis (PERMANOVA, R function "adonis", R-package "vegan") (Oksanen et al., 2008). Identification of features differentially abundant between samples was performed by random forest classifier and differential expression analysis based on the Negative Binomial (a.k.a. Gamma-Poisson) distribution (R function "differential_abundance" in R-package "MicrobiomeSeq", https://github.com/umerijaz/microbiomeSeq). Mean decrease in accuracy (the decrease of accuracy due to the exclusion of a specific feature) was used to evaluate the importance of the feature.

### 2.3. Sample preparation and mass spectrometric analysis

Approximately 180 mg fecal samples were suspended in water, a subsample of each was mixed with acetonitrile to a final concentration of 1% and acidified with formic acid to a final concentration of 0.5% to counteract the buffer capacity of the samples. Samples were filtered on 3000 Da Amicon Spinfilters to remove debris. The samples were analyzed by liquid chromatography tandem mass spectrometry (LC-MS/MS) and data was recorded in a data dependent manner, on a Q-Exactive (Thermo Scientific, Bremen, Germany). An EASY nLC-1000 liquid chromatography system (Thermo scientific, Odense, Denmark) was coupled to the mass spectrometer through a 2 cm C18 pre-column (300 µm inner diameter, 1.9 µm particle size) and a self-packed 15 cm C18 column (Pico Frit columns from New Objective) with a 75 µm inner diameter, packed with (1.9 µm C18 Dr. Maisch Mat. No. r119.a). Metabolites were eluted with a mobile phase consisting of solvent A (0.1% formic acid) and B (80% acetonitrile in 0.1% formic acid). The concentration of solvent B was linearly increased from 2 to 10% over 3 min and from 10 to 95% solution B over 15 min. Solvent B was maintained at 95% for 2 min. Full scans were acquired in the Orbitrap with a resolution of 70,000, maximum injection time of 20 ms and a scan range of 80–1200 *m/z* using a Top 10 method with an isolation window of 1.6 Da and a dynamic exclusion time of 15 s. For the MS/MS scans the resolution was adjusted to 17,500 and maximum injection time of 60 ms. Ions were fragmented with a normalised collision energy (NCE) of 30%.

### 2.4. Metabolomics processing and analysis

LC-MS/MS raw data files were converted to .mzXML using msconvert from ProteoWizard (v. 3.0) and preprocessed using MZmine 2.3 (Pluskal et al., 2010) with parameters set to Peak detection, Mass detection, Mass detector: Centroid, MS1 noise level 2.0E5, MS2 noise level 100; Chromatogram builder: MS1 level, Min time span (min) 0.01, Min height 6.0E5, *m/z* tolerance 0.01 Da or 10 ppm; Chromatogram deconvolution: Algorithm Local minimum search, Chromatographic threshold 90%, Search minimum in RT range (min) 0.01, Minimum relative height 10%, Minimum absolute height 1000, Min ratio of peak top/edge 1.3, Peak duration range (min) 0.01–10.00, *m/z* range for MS2 scan pairing (Da) Off, RT range for MS2 scan pairing (min) Off; Isotopic peak grouper: *m/z* tolerance 0.01 Da or 10 ppm, Retention time tolerance 0.5 (min), Maximum charge 4, Representative isotopes Most intense; Feature alignment: *m/z* tolerance 0.01 Da or 10 ppm, Weight for *m/z* 75, Retention time tolerance 0.5, Weight for RT 25; Gap filling: Intensity tolerance 10%, *m/z* tolerance 0.01 *m/z* or 10 ppm, Retention time tolerance 0.5 (min), RT correction Off. Mass spectral molecular networks (Watrous et al., 2012) were created by uploading the MZmine preprocessed .mgf file to the Global Natural Products Social Molecular Newtorking platform (GNPS) (Wang et al., 2016) with parameters described at https://gnps.ucsd.edu/ProteoSAFe/status.jsp?task=806fa2cdc63b41f59b17b59e2a5da0ee.

Before statistical analysis, features not found in a minimum of 20 samples were filtered out, reducing dimensions from 8562 to 2130. Upon visual inspection of a PCA plot of all samples, Sample36 (Cd group) were discarded as an outlier. The best performing univariate statistical test were determined using the R-package "DAtest" (https://github.com/Russel88/DAtest) with default settings. The *t*-test performed the best in terms of controlling the false positive rate at 0.05, while having the best ROC of the methods tested. The tests were then performed using the R function "DAtest.tte", and evaluated by the FDR corrected *p*-values, with 0.05 deemed significant. PCA analysis was done using the R function "prcomp" on square root transformed features. Multivariate hypothesis testing was performed using the R function "adonis" in R-package "vegan" (2.4-4) (Oksanen et al., 2016) with the Euclidian distances of square root transformed features.

To putatively identify molecular features, we used both GNPS library matching as well as *in silico* structure annotation by the Network Annotation Propagation (NAP) tool (da Silva et al., 2018). Due to the aforementioned interest in bile acids, we submitted a user provided database to NAP. This database was compiled by downloading all metabolites in the "Bile acids and derivatives [ST04]" category of LIPIDMAPS and is publically accessible at Additional file C. NAP parameters are described and can be accessed at: https://proteomics2.ucsd.edu/ProteoSAFe/status.jsp?task=a1c0ebb9ec2943ddbf0ff242c622f35e

https://proteomics2.ucsd.edu/ProteoSAFe/status.jsp?task=4844738f1edb4c4d9a836abdc9cd5820

https://proteomics2.ucsd.edu/ProteoSAFe/status.jsp?task=232cf5a822864a31aeb0603b957c11c2

### 2.5. Concordance analysis

Correlations between OTUs and metabolites were calculated using the R function "protest" in the R-package "vegan" (2.4-4) (Oksanen et al., 2016).

### 2.6. Integrative network analysis

Integrative network analyses were performed in R. Pearson correlations were calculated for a bipartite network of OTUs and metabolites using a Fisher transformation, and correlations at the 0.05 FDR level were included (Kolaczyk et al., 2014). Both OTU and metabolite tables were pruned for near zero variance features, using the NearZeroVariance function from the "caret" package (Kuhn, 2008). Networks were managed and visualized in the R-package "igraph" (1.2-2) (Csardi, 2015). Differential networks were calculated using fishers transformation of correlation coeffecients as shown in the R-package "Diffcorr" (Fukushima, 2013). Briefly, a network of Pearson correlations was calculated for each condition (control, As and Cd treatment), where links were defined by significant correlations after FDR adjustment. The difference in correlations (r) between samples A and B are then calculated by transforming each coefficient into a *Z*-score (Z) by $Z_A = 0.5 * \log\left(\frac{1+r\_A}{1-r\_A}\right)$ And calculate the differential score as $Z = \frac{Z_A - Z\_B}{\sqrt{\frac{1}{n_A-3} + \frac{1}{n_A-3}}}$, *p*-values were calculated assuming a normal distribution. Taxa enriched in differential links were identified by permuting the taxa label 100 times and performing a one-sided evaluation. Adjustment for permutation *p*-value misestimation was applied (Phipson and Smyth, 2010). To further avoid false positives all taxa with prevalence lower than 1/3 presence in the condition were set to 0.

## 3. Results

### 3.1. Sequencing summary and phenotype assessment

The experimental workflow combining 16S rRNA gene sequencing and metabolite profiling to test the impact of As and Cd exposure on the gut microbiome and its metabolism, is shown in Fig. 1. The V3-V4 region of 16S rRNA gene amplicons from fecal samples from a total 31 subjects (control group ($n$ = 13), As group ($n$ = 7), Cd group ($n$ = 11))

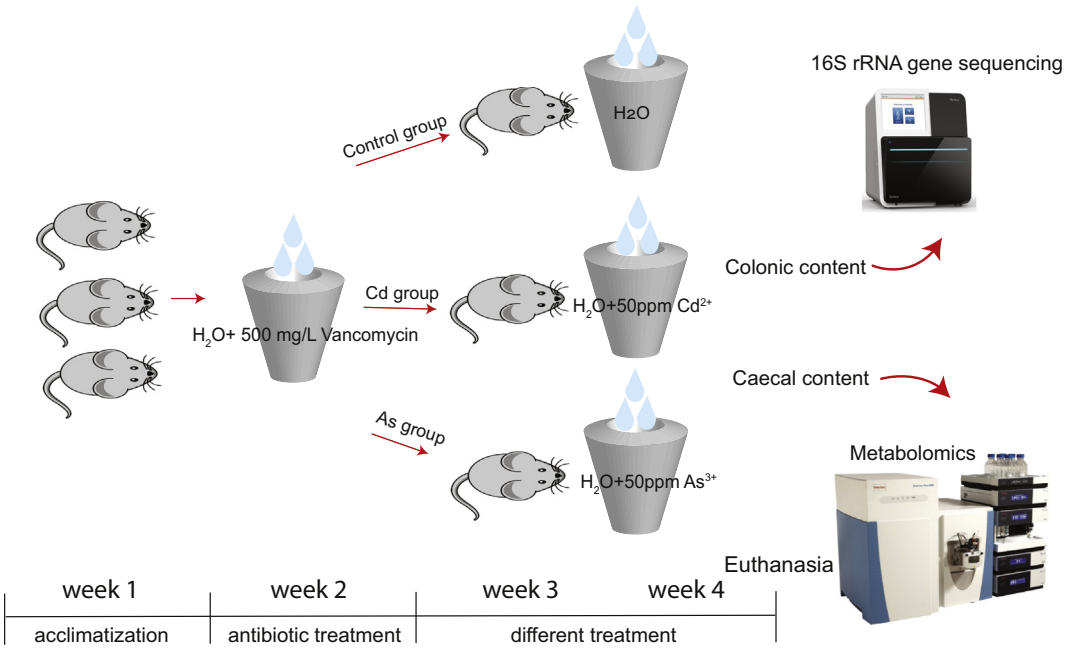


**Fig. 1.** Flow chart of this study. A total of 48 mice were included in this study. Water and food was available ad libitum during the whole experimental period. Mice were treated with 500 mg/L vancomycin in the drinking water during the second week after the initial adaption to cage-food and laboratory conditions during the first week. Then, the mice were randomly divided into 3 experimental groups. One group, serving as the control drank water free of contaminants, and the other two groups were separately treated with 50 ppm $CdCl_2$ or 50 ppm $NaAsO_2$ supplied in the drinking water for two weeks. All mice were euthanized after anesthetization with ether on the last day of the treatment. Colon and caecum contents were collected for 16S rRNA gene sequencing and metabolomics respectively.

(14 samples missing because of no amplification) were sequenced using the Miseq PE300 platform. The average sequencing depth obtained for the 31 subjects was 142,807 reads per sample, which was reduced to 62,498 (SD = 24,455) high quality sequences after QC. Body weight, food and water consumption during the experiment for all the groups did not differ significantly, as shown by Wilcoxon Rank Sum test (see Tables S1 and S2).

### 3.2. Exposure to cadmium significantly altered the gut microbial diversity

In order to investigate the changes in gut microbial community triggered by the different treatments, we compared the microbial diversity of the different treatment groups. As shown in Fig. 2A, we found that both treatments caused a decrease in diversity of the gut microbiome, but only to a significant degree in the Cd treated mice ($p = 0.028$). A clear distinction was also observed between the microbial communities of the control group and the Cd group, as shown in the PCoA plot (Fig. 2B). The control and treated mice were significantly separated, with 42.6% and 22% variation explained by principle component PC1 and PC2, respectively. The Cd treatment explained 25% of the variance ($p = 0.003$), while the As treatment explained 2% of the variance ($p = 0.8$). No significant differences in microbial diversity were observed between the As group and the control group (Fig. 2B).

### 3.3. Heavy metals induced significant changes in the gut microbiome

The four major phyla composing the microbial community are listed in Fig. 3A. The phylum Verrucomicrobia mostly composed of the genus *Akkermansia*, was the second most abundant phylum, verifying the enrichment effect of vancomycin on gram-negative bacteria.

A random forest classifier approach was used to explore the specific

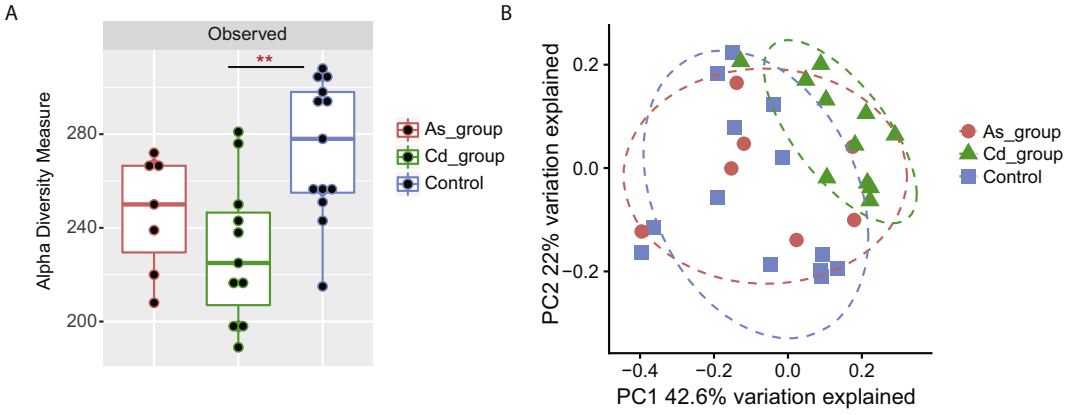


**Fig. 2.** Variability in community composition between and within samples. (A) Variation in diversity within the three groups. Sample diversity was measured at the OTU level (> 97% identity). The microbial community in the control group displayed a significantly higher diversity than that displayed in the Cd group (Tukey HSD; $p = 0.0028$** for Observed richness), and somewhat higher than that displayed in the As group, although not significant. (B) Microbial clustering based on the Weighted-Unifrac distance metric, visualized by principle coordinate analysis. (PERMANOVA; $R^2 = 0.26085$, $p = 0.003$** for the Cd group vs. control).

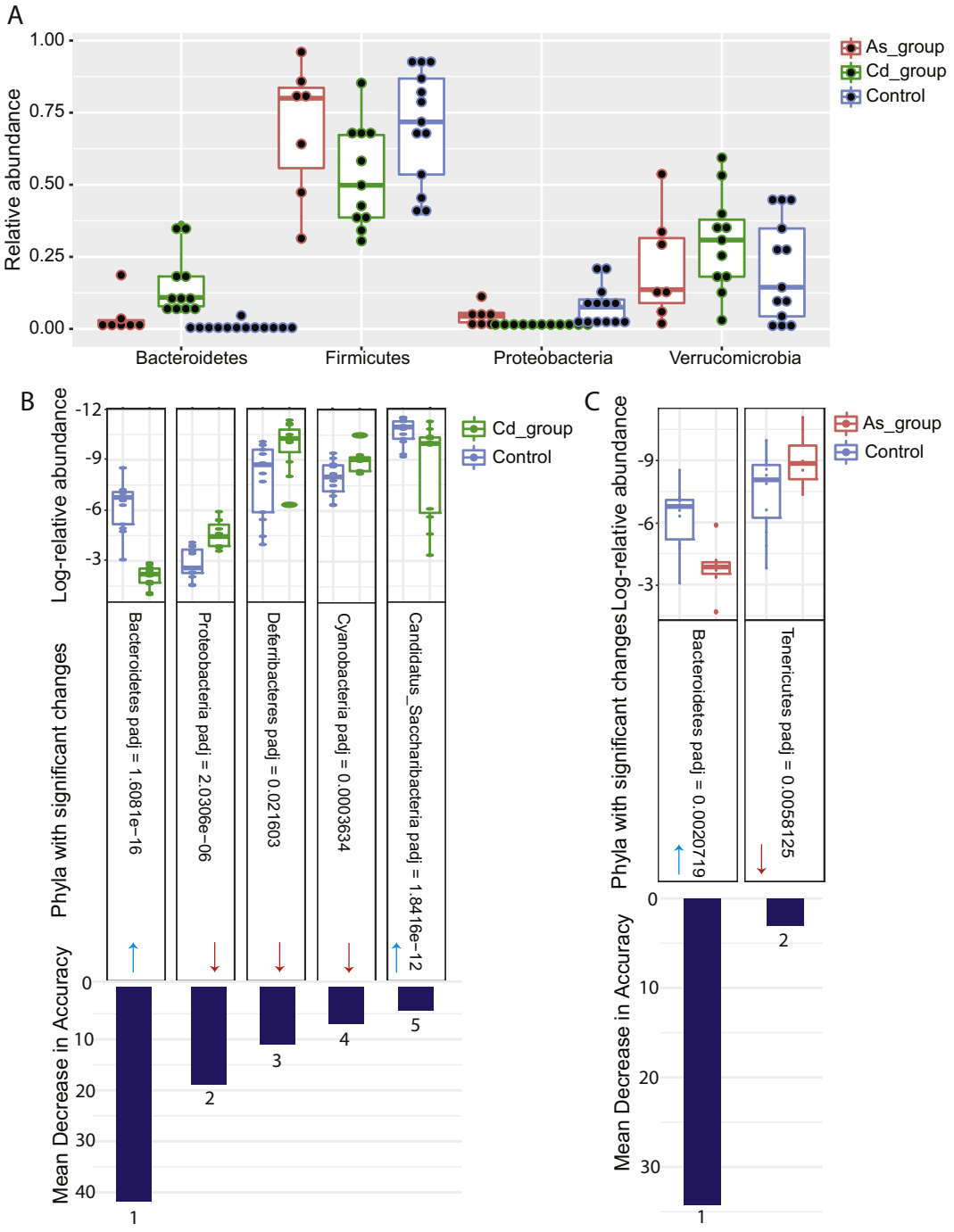


**Fig. 3.** (A) Distribution of phyla between experimental groups. (B,C) Significantly differentially abundant phyla between Cd (B)/As (C) and control group: The boxplots are the log relative normalised abundances for the treatment groups. The bar plot correspond to importance of a corresponding feature based on mean decrease accuracy and on bottom of which the ranks are indicated. The middle section of the plot shows phyla description and corresponding adjusted *p*-value. The arrows inside the middle section of the plot indicate the upregulation (blue arrow) or downregulation (red arrow) of the corresponding phylum abundance (Cd/As vs Control). (For interpretation of the references to colour in this figure legend, the reader is referred to the web version of this article.)

changes in the gut microbiome caused by the different treatments. Two phyla in the As group and five phyla in the Cd group were differentially abundant compared to the control group (Fig. 3B and C). In both groups, *Bacteroidetes* rank first in importance by the random forest classifier analysis. The abundance of *Bacteroidetes* was significantly higher in the control group as compared to both As ($p$ = 0.002**) and Cd ($p$ = 1.6e-16***). *Proteobacteria* in the Cd group and *Tenericutes* in the As group were less abundant than in the control group ($p$ = 2.03e-06*** and $p$ = 0.006** respectively). In addition, the abundance of *Deferribacteres*, *Cynaobacteria* and *Candidatus_Saccharibacteria* in the Cd group showed significant differences from the control group. Further information about these significantly changed phyla has been listed in Tables S3 and S4. Fold changes for all phyla in both groups are shown in Fig. S1. At the genus level, 24 genera in the As group and 42 genera in the Cd group were differentially abundant as compared to the control group (Figs. 4 and 5), with 15 and 24 being downregulated respectively (Tables S3 and S4). Most of the significantly changed genera belonged to the phyla *Firmicutes*, *Bacteriodetes* and *Proteobacteria* (Figs. 4 and 5). Specifically the *Clostridiales* order within the *Firmicutes* phylum accounted for 14 of the 24 different genera in the As group and 24 of the

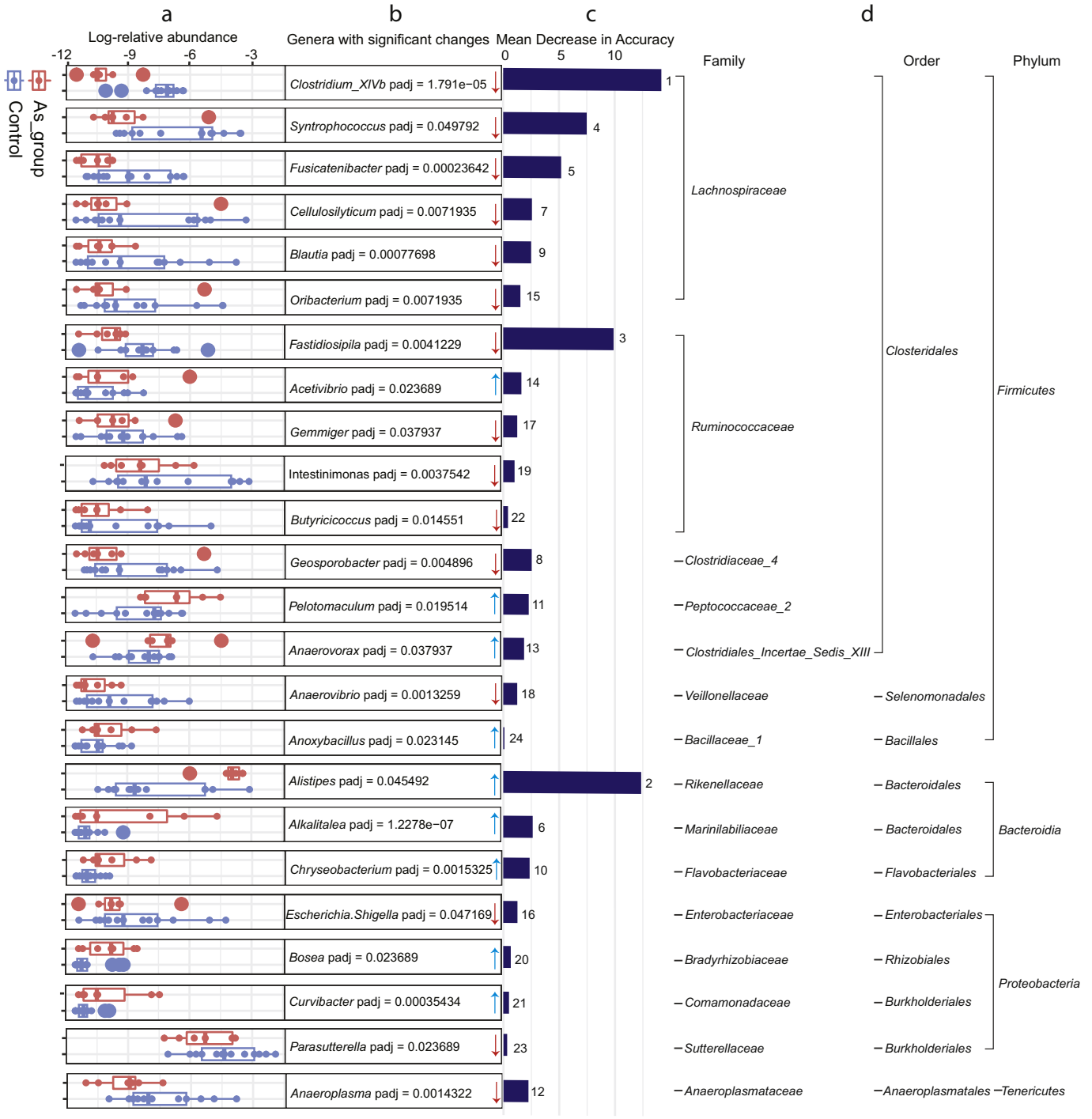


**Fig. 4.** Significantly differentially abundant genera between As and control group: a. The log relative normalised abundances for the treatment groups. b. The genera description and corresponding adjusted *p*-value. The arrows inside the second section of the plot indicate the upregulation (blue arrow) or downregulation (red arrow) of the corresponding genus abundance (As vs Control). c. The importance of a corresponding feature based on mean decrease accuracy and on right of which the ranks are indicated. d. The taxa information of the corresponding genus. (For interpretation of the references to colour in this figure legend, the reader is referred to the web version of this article.)

42 different genera in the Cd group. Further, 9 of the downregulated genera (*Clostridium_XlVb*, *Syntrophococcus*, *Cellulosilyticum*, *Blautia*, *Anaeroplasma*, *Gemmiger*, *Anaerovibrio*, *Intestinimonas*, *Parasutterella*) and 2 of the upregulated genera in both groups (*Alistipes* and *Alkalitalea*) showed overlap between the As and Cd groups. Additional information for the significantly changed genera has been listed in Tables S3 and S4. Fold changes for all the genera in both groups have been shown in Fig. S2.

Due to the vancomycin treatment, which resulted in accumulation of gram-negative gut bacteria, *Akkermansia* was the most abundant genus in both groups (Fig. S3). Despite detected high sensitivity to As and Cd *in vitro* (Fig. S4), only the As group showed a decrease in abundance of *Akkermansia* (1.8 fold) whereas the Cd treatment showed a surprising 1.25 fold increase.

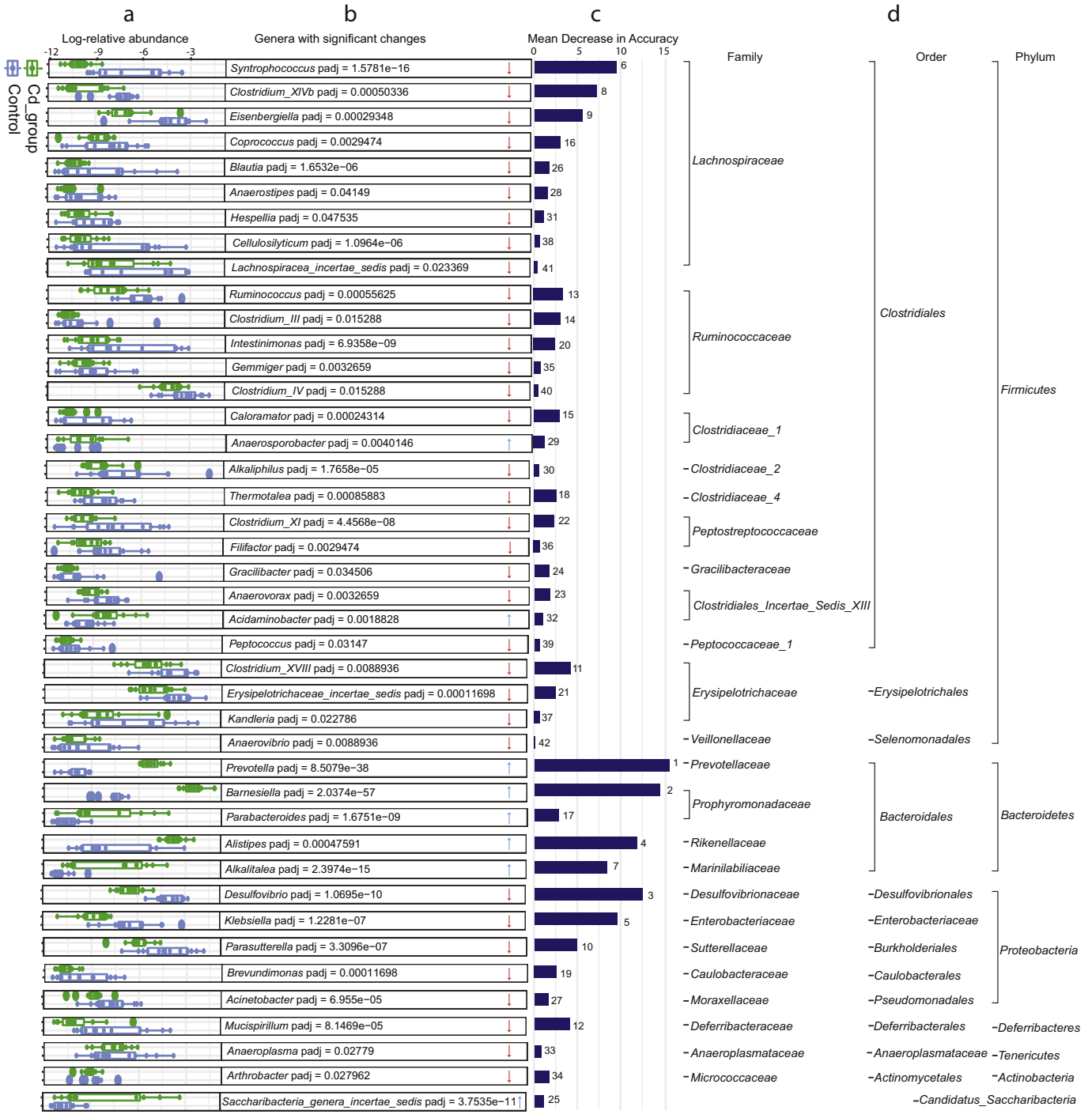


**Fig. 5.** Significantly differentially abundant genera between Cd and control group a. The log relative normalised abundances for the treatment groups. b. The genera description and corresponding adjusted *p*-value. The arrows inside the second section of the plot indicate the upregulation (blue arrow) or downregulation (red arrow) of the corresponding genus abundance (Cd vs Control). c. The importance of a corresponding feature based on mean decrease accuracy and on right of which the ranks are indicated. d. The taxa information of the corresponding genus. (For interpretation of the references to colour in this figure legend, the reader is referred to the web version of this article.)

### *3.4. Heavy metals induced global changes in the gut metabolome*

Metabolomic profiles of the fecal contents were generated using liquid chromatography coupled to tandem mass spectrometry (LC–MS/MS), including16 control samples, 13 As group samples and 15 Cd group samples. Mass spectral molecular networks (Watrous et al., 2012) were created using the online Global Natural Products Social Molecular Networking platform (GNPS) (Wang et al., 2016). Processing of spectra resulted in 26,978 features for all the samples. Rarefaction curves of feature richness showed little difference between the As and control groups, but there were fewer observed features in the Cd group (Fig. S5-A). Multivariate differences between treatment and control were assessed using PERMANOVA and PCA. The As treatment explained 5.1% of the variance in the metabolome ($p = 0.0456$*), while the Cd treatment explained 7% of the variance ($p < 0.001$***). PCA analysis (Fig. 6) visually separated the different groups. Both treatments induced the presence of features not found in the controls. Cd treatment showed 111 uniquely present features while As treatment showed 11.

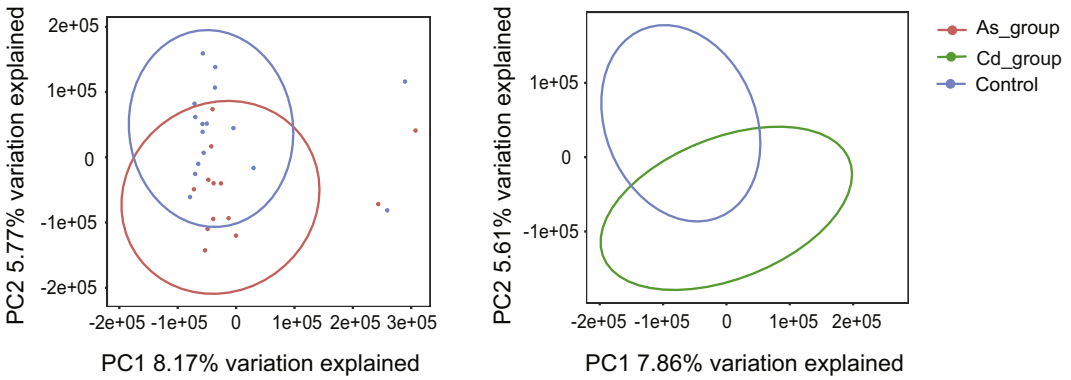


**Fig. 6.** PCA analysis of metabolome profiles from As vs Control (A) and Cd vs Control (B). The two treatment groups displayed significant differences from the control group (PERMANOVA, $p = 0.0456$ for As group, $p < 0.001$for the Cd group). The As treatment explained 5.1% of the variance in the metabolome, while the Cd treatment explained 7% of the variance.

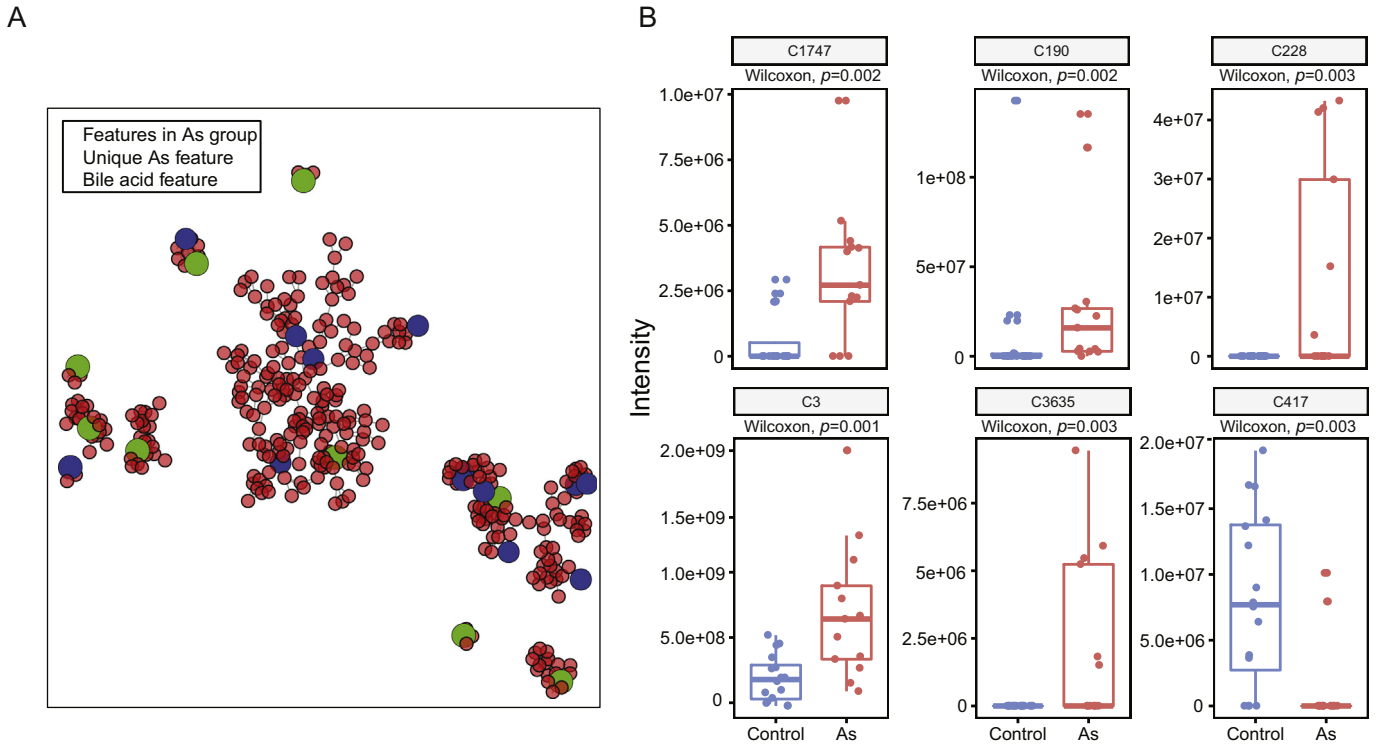


**Fig. 7.** Bile acid analysis of the metabolome. (A) Investigation of features uniquely found in As treated mice revealed that most were found in molecular families associated with bile acids according to a GNPS library search, implying they were structurally related to bile acids. (B) An *in silico* search via NAP using a specialized bile acids database identified a number of bile acid related molecular components. These were tested for differential abundance, and the significant ones were plotted. Most of the components showed an increase under As treatment.

Closer inspection of the molecular network showed that many unique features from the As treatment were associated with bile acid molecular families (Fig. 7A). The recorded *m/z* values of the nodes within each network was quite homogenous, providing additional evidence for the molecular relatedness.

To identify differentially abundant features, a *t*-test was performed for every feature in each group and *p*-values were corrected for multiple hypothesis testing. This resulted in 2 and 33 features identified as significantly different in the As and Cd group, respectively (Table S5 and Fig. S5-B). Neither of the two As features could be identified based on MS2 fragmentation spectra. Several differentially abundant features in the Cd exposure group were putatively identified through a GNPS library search. Among these were several amino acids such as valine, aspartic acid, methionine, and tyrosine, as well as the non-standard amino acid norleucine. Finally one feature matched to alpha-Cyano-4-hydroxycinnamic acid, and manual inspection of the spectra confirmed this. The latter being strongly decreased in the treated mice with a log fold change of −15.

### 3.5. Heavy metals induced changes in the bile acid fraction of the metabolome

Due to the bile acids associated molecular networks unique to As treatment, we putatively annotated the bile acid fraction of the fecal metabolome using *in silico* structure annotation through the recently available Network Annotation Propagation algorithm (NAP). All metabolites in the “Bile acids and derivatives [ST04]” category of LIPID-MAPS were downloaded and fragmented *in silico* to compare with the acquired fragmentation spectra. This identified 633 features as bile acid related. In the previously constructed molecular network they were

distributed in 181 different molecular families (two or more connected molecular signatures). Aggregating the intensities of these components, we created a boxplot to show differentially abundant (DA) molecular families of putative bile acid molecules in the As group (Fig. 7B). We identified 6 DA molecular families in the As treatment and 2 DA molecular families in the Cd treatment. The intensities of 5 DA bile acid molecular families in the As group elevated but one DA bile acid molecular family decreased.

### 3.6. Bipartite interaction network identified bacteria-metabolite interactions in Cd associated bacteria

We examined the concordance between metabolite and microbiome data by Procrustes correlation which was significant (protest, correlation = 0.65, $p = 0.006$), suggesting that a fraction of the fecal metabolites are substrates or products of the microbiome.

To further investigate how this connection might change upon heavy metal treatment, bipartite correlation networks were created from the paired microbiome-metabolome tables. This resulted in three networks (not listed), of which the control treatment had the fewest interactions and the Cd treatment had by far the most interactions, despite the Cd-treated mice metabolomes having the fewest detected features. To identify the effects of the treatment on these networks, differential networks in which the difference in correlations between control and treatment were calculated. At the same time, a permutation test was applied to compare the number of changed links to the null hypothesis of random changes to identify genera with potential changed metabolic output. Correspondingly, we identified a number of significant metabolite interactions within each genera from these networks.

Several genera with significant changes in the number of metabolite interactions were identified. We found 7 genera which presented significant changes to their differential networks in the Cd treatment and 3 under the As treatment. *Clostridium_XlVa* had a large amount of changes in both treatments. All differential correlation networks are presented in Fig. 8. While the genera had overall significantly different interaction patterns, there were clear within-genus differences at the OTU level. Fig. 8 illustrates *Blautia* metabolic interaction changes, while OTU_7 primarily increased interactions, OTU_356 clearly decreased its interaction strengths with many metabolites. In other cases such as *Eisenbergiella*, several OTUs regulated their interaction with several metabolites in both treatments, suggesting a shared response to the treatment. The differential network for the two *Anaerostipes* OTUs under cadmium treatment is entirely disconnected.

## 4. Discussion

The current experiment was set up to connect the associations from the epidemiology literature concerning induction of type II diabetes with the observations from the microbiome literature, and hopefully narrow the role of the metabolome. In this study we hypothesized that Cd and As treatment would change the gut microbiome in mice. The hypothesis was tested using a combination of 16S rRNA gene sequencing and liquid chromatography coupled to tandem mass spectrometry (LC-MS/MS) metabolomics. This was done on three groups of mice which were administered either cadmium chloride or sodium arsenite in their drinking water after treatment with vancomycin. We demonstrated that the exposure to toxic metals such as Cd and As resulted in different gut microbiomes and metabolomic profiles in mice. In the present study, we added the same dose of 50 ppm $CdCl_2$ and $NaAsO_2$ in the drinking water of treated mice. 50 ppm $CdCl_2$ and $NaAsO_2$ contain 0.273 mmol/L $Cd^{2+}$ and 0.385 mmol/L $As^{3+}$, respectively. During Cd/As exposure period, the volume of drinking water for the three experimental groups did not show significant differences (Wilcox test, $p > 0.05$), hence mice in the Cd group ingested less molarity of $Cd^{2+}$ than mice in the As group within 2 weeks. Even so, overall, the changes in composition of the gut microbiome and metabolome perturbation were qualitatively and quantitatively greater in mice exposed to Cd than in the mice exposed to As. The effect size (R-squared value) of the PERMANOVA test suggested that the impact of Cd treatment was larger on the gut microbiome and metabolome. Accordingly, 24 genera were detected to be differentially abundant after the As exposure while 42 genera were significantly different in abundance in Cd treated mice. Furthermore, 33 metabolic features were found to be significantly differentially abundant after Cd treatment, and only two in the As group. We speculate this is likely due to the differences in detoxification mechanisms of the host to the two compounds, ultimately reflected in the feces metabolome. Under the long-term exposure, Cd ion is more difficult to be cleared *in vivo* due to high stability and the lack of sound detoxification mechanism. In contrast, As is cleared from the body by methylation to its mono or di-methylated forms and 70% of this water-soluble form can be transported and excreted in the urine (Keil et al., 2011). In addition, the biological half-life of inorganic arsenic is about 4 days (NRC, 1999). However, Cadmium is bound to albumin and transported to the liver, bound to metallothioneins and finally transported to the kidney where its halflife could be decades (Suwazono et al., 2009). The Cd accumulation the kidney from Cd exposure likely mediates the downstream effects of the fecal metabolome more than acute exposure of the microbiome to bioavailable Cd.

Lu et al. previously conducted a more general intervention study with As (Lu et al., 2014), but we did not find much overlap between results. The present study was focused primarily on gram-negative bacteria with a pre-intervention vancomycin treatment. While this induces a dysbiotic microbiome it nevertheless allows highlighting the gram-negative fraction hypothesized to be relevant for the ethiology of T2DM. Yet, there were still some overlapping findings for taxa in *Clostridiales*, but overall this strategy did not induce a difference in the microbiome as reflected by multivariate analysis. Similarly there was a small overlap in the metabolome, and more fatty acids were detected in Lu et al., possibly due to methanol extraction rather than water as in the present study.

The tendency of significantly decreased microbial diversity in the Cd group and reduced microbial diversity in the As group observed in this study (Fig. 2), indicated that the response to toxic metals pose an adverse challenge to many gut bacteria. The relative abundances of *Bacteroidetes* in the Cd and As groups were significantly higher compared to the control group (Fig. 3), and the relative abundance of *Proteobacteria* in the Cd group was significantly lower. The trends regarding change in abundance for these two phyla are supported by current studies relevant to Cd (Breton et al., 2013; Liu et al., 2014; Zhang et al., 2015). At the genus level, bacterial groups that were significantly different in the As and Cd group compared to the control group included 24 and 42 genera, respectively (Figs. 4 and 5), of which 9 and 8 genera were positively correlated to As and Cd exposure, respectively. Among these upregulated genera, the importance of *Barnesiella*, *Alistipes*, *Alkalitalea*, *Prevotella* ranked at the top and especially *Alistipes* and *Alkalitalea* were found in both groups. Literature is very limited on the association of *Alkalitalea* and T2DM, but the change in *Alkalitalea* abundances, a 53-fold decrease in the As group and a 137-fold decrease in the Cd group, is noteworthy. *Barnesiella* and *Alistipes* were previously shown to be reduced after treatment for T2DM (Hansen et al., 2012; Xu et al., 2015). Further, a decrease in *Parabacteroide and Prevotella* were reported after probiotic yeast treatment (Yu et al., 2017) and therefore seemingly associated with T2DM (Wu et al., 2010; Xu et al., 2015), which supports our results. Certain strains within the other upregulated genus *Chryseobacterium* have been reported as rare pathogens in humans and had also been found in diabetic children (Cascio et al., 2005). Among the genera negatively correlated to As and Cd exposure, the sulphate-reducing bacteria (SRB) *Desulfovibrio* were identified as the most important genus in the Cd group by Random forest classifier. New research has showed that SRB was accompanied by enhanced glucagon-like peptide 1 and insulin secretion, which

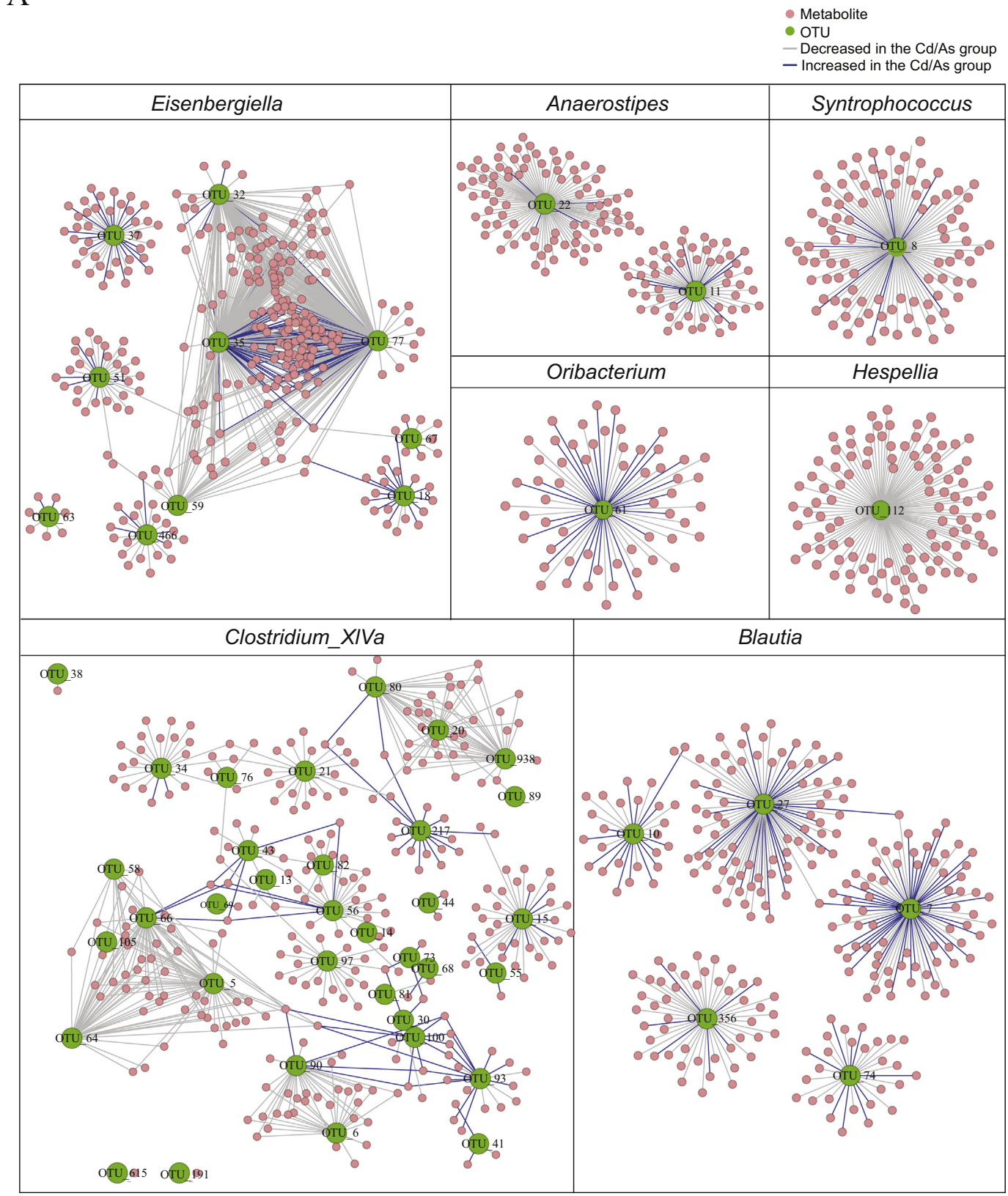


**Fig. 8.** Integrative bipartite networks. Networks of Pearson's correlations were calculated to investigate interactions between OTUs and metabolites. (A) Genera with significantly changed numbers of interactions under the Cd treatment (adjusted $p < 0.01$, the connections with the absolute value of weights below 5 in the genus *Clostridium*_XIVa were filtered out). (B) Genera with significantly changed numbers of interactions under the As treatment (adjusted $p < 0.01$, the connections with the absolute value of weights below 5 in the genus *Clostridium*_XIVa were filtered out). *Eisenbergiella*, *Blautia and Anaerostipes* have several OTUs, some of which display a finer scale structure.

B

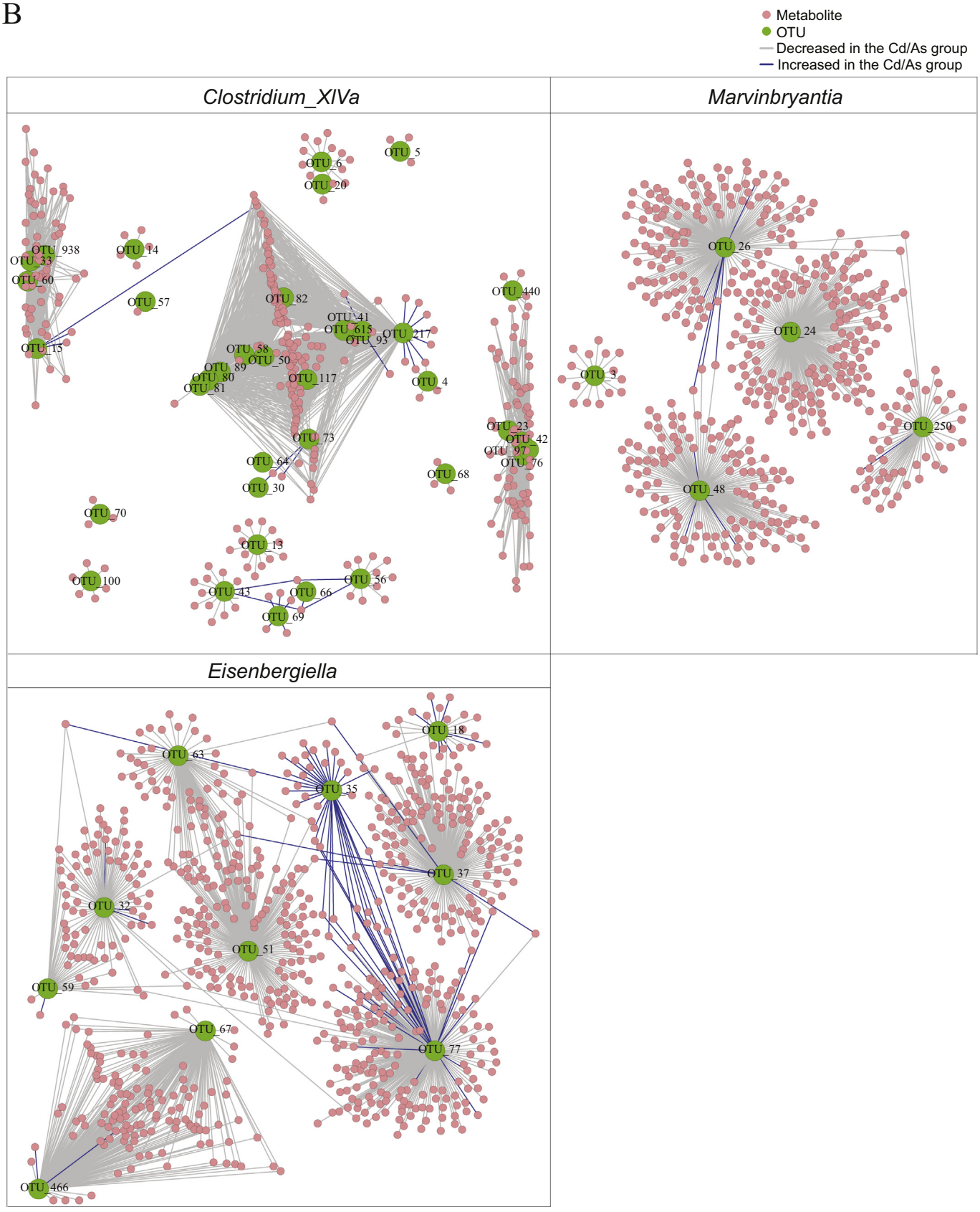


**Fig. 8.** (*continued*)

further improved oral glucose tolerance and reduced food consumption (Pichette et al., 2017). We also found that a series of genera belonging to the butyrate-producing superfamily *Lachnospiraceae* within the order *Clostridiales* that were downregulated in both groups, which included *Fusicatenibacter*, *Eisenbergiella*, *Syntrophococcus*, *Blautia*, *Clostridium_XIVb*, *Cellulosilyticum*, *Oribacterium*, *Coprococcu*, *Anaerostipes*, *Hespellia*, *Cellulosilyticum* and *Lachnospiracea_incertae_sedis*. Besides, the relative abundances of some genera belonging to family *Erysipelotrichaceae*, which is distantly related to *Lachnospiraceae*, *Clostridium_XVIII*, *Kandleria* and *Erysipelotrichaceae_incertae_sedis*, were decreased in the treatment group. Butyrate produced by gut bacteria is a major energy source for the colonic epithelium (Roediger, 1980) and could improve insulin sensitivity and increase energy expenditure (Gao et al., 2010). Besides, genera within butyrate-producing families, the other downregulated genera shared by the As and Cd groups, such as *Parasutterella* and *Gemmiger*, have also been associated with alleviation of T2DM (Xu et al., 2015).

*Akkermansia* was not as sensitive to Cd and As *in vivo* as in *in vitro* experiments. Although the relative abundance of *Akkermansia* was higher in the Cd group and lower in the As group, the changes were not substantial and not statistically significant. We assumed that the intestinal microbial consortia tend to be cooperative (Bäckhed et al., 2005) and this could further weaken the adverse effects from exogenous metals on a single species, which may explain the different results *in vivo* and *in vitro*. Some bacteria with probiotic properties such as *Faecalibacterium* and *Bifidobacterium* which have displayed beneficial effects on glucose metabolism in humans (Cani et al., 2009; Hill et al., 2014; Miquel et al., 2014) were also detected in our study. In accordance with these outcomes, both *Faecalibacterium* and *Bifidobacterium* decreased slightly in the Cd and As groups.

Despite large improvements in LC-MS/MS library searching technology and expansion of the libraries, identifying features is still not perfect, and overall in this study we could identify 3770 library hits out of 26,978 features (13.9%) using the GNPS platform. Previous summaries on the studies of metabolomics have estimated an average of 2% identification rates of features (Aksenov et al., 2017). One advantage of using the GNPS platform is that the data is continuously being updated with improved annotations (Wang et al., 2016). Of the differentially abundant features identified from the Cd group, several of them could be annotated as amino acids through library matching. It is well-established by serum metabolomics that the concentrations of amino acids change in T2DM subjects. This applies to amino acids in general (Guasch-Ferré et al., 2016), but branched chain amino acids (BCAAs) have, in particular, been associated with insulin resistance, and the microbiome has been demonstrated to contribute to the increased concentrations of amino acids in serum (Pedersen et al., 2016). At present, the causal path to insulin resistance remains unclear with Mendelian randomization studies suggesting that insulin resistance preceded increased BCAA levels (Mahendran et al., 2017). However, this accounts only for the variation caused by genetics. Additionally, it is unclear how amino acid levels in feces translate to amino acid levels in serum. A previous study observed that the main site of murine amino acid metabolism was higher in the gastro-intestinal tract, peaking in the jejunum (Heinzmann and Schmitt-Kopplin, 2015), possibly blurring the observations of caecal amino acids.

There are a limited number of feces metabolomic studies in T2DM but high-fat diet fed mice are known to have higher levels of tyrosine in fecal metabolomic phenotyping using an untargeted NMR investigation (Lin et al., 2016), which are consistent with our observations in the present study. In addition, in the present study, the abundance of 4-hydroxycinnamic acid which is an intermediate of several pathways, including the degradation of tyrosine deceased significantly by 15 fold in the Cd group. Tyrosine in blood has previously been identified as increasing the T2DM risk in a meta-analysis of 8000 metabolomic samples (Guasch-Ferré et al., 2016). In the present study, there was an increase in valine abundance after Cd exposure. Serum valine in humans has been linked to the visceral deposition of fat which has strongly been suggested to drive insulin resistance (Lebovitz and Banerji, 2005; Schlecht et al., 2017). Previous studies on insulin resistant rats using NMR showed consistent longitudinal increases in isovalerate (Yang et al., 2015), a degradation product of valine (Zarling and Ruchim, 1987). A metabolomics study of beta-cell function in insulin secretion had previously identified intracellular norleucine levels as statistically associated with insulin secretion (Huang and Joseph, 2014). However, connecting this finding to the fecal content would require a further investigation of the norleucine homeostasis.

We specifically chose to focus on the fraction of the metabolome that could be assigned to bile acids, as changes in this fraction has previously been associated with metabolic problems in humans. Additionally, it had been shown that microbes can actively manipulate this fraction of the metabolome by making an array of chemical modifications that alter the potency of the impact of a bile acid. Bile acid concentrations have been correlated with the microbiome in germ free mice (Claus et al., 2008) and shown implications in obesity in feeding studies (Lin et al., 2016; Walker et al., 2014). Our results displayed a change in features of the bile acid fraction of the metabolome. These findings should be followed up with more targeted metabolomics to identify the exact molecular identities of the bile acids.

We built the integrative networks to identify exactly which OTUs had altered interactions with the metabolites, as it has been hypothesized that deteriorating metabolic health is mediated through microbiome interaction with the metabolites, either through production or through consumption. We demonstrated that certain genera seem to have enriched or lowered metabolic interactions. This is particular noteworthy for the genera, *Blautia*, which had also been highlighted in previous literature for their metabolic capabilities, that showed a large number of interactions in the control network, but had a decreased number of interactions in both treatments. Similarly, *Anaerostipes* species had been shown to aggravate DSS induced colitis, presumably through its metabolic output (Zhang et al., 2016). These genera have been implicated in several types of metabolically related human health issues, presumably because of their butyrate producing capacity. In addition, the relative recently isolated genus *Eisenbergiella* displayed significant interactions after both treatments. The interaction networks at the OTU level made it clear that there were finer scales of interactions, with certain OTUs losing many interactions and some showing no difference under treatment conditions. This will be a starting point for a more targeted investigation at the species/strain level and for the metabolites that could reveal the exact interactions.

## 5. Conclusion

We have conducted an exploratory feeding study in mice to investigate the impact of heavy metals mainly on the fecal gram-negative bacteria enriched by Vancomycin and its metabolome to validate the hypothesis generated from epidemiology and cell culture studies that heavy metals can impact host metabolic health. Heavy metals do indeed impact both microbiome and metabolome, without substantially affecting the phenotypes of the mice. Cadmium exposure significantly changed the mice gut microbiome as well as resulting in a significantly lower microbial diversity in the gut. Arsenic exposure resulted in a lower microbial diversity, although not significant. By using untargeted technologies for observing microbiome and metabolites, we observed several metabolically health related microbes differentially abundant in the As and Cd treatment groups. When examining the metabolites we could see an impact of both Cd and As treatment on both amino acids and bile acids. Further studies must elucidate how these results relate to the serum metabolome and ultimately impact human health. Finally, we studied microbiome-metabolite interactions based on the assumption that the health impact of the microbiome is mediated by their metabolites. We demonstrated substantial changes for genera that have previously been implicated in disease outcomes specifically because of

their metabolites. More research is needed to clarify the exact nature of these metabolites and their impact.

Supplementary data to this article can be found online at https://doi.org/10.1016/j.envint.2019.02.048.

## Ethics approval and consent to participate

The animal research was approved by China National Accreditation Board for Laboratories and China Food and Drug Administration (Ethical approval number: BLARC2015A1203).

## Consent for publication

Not applicable.

## Availability of data and materials

The 16S rRNA gene sequencing dataset analyzed during the current study are available, upon publication, in the Sequence Read Archive (SRA) repository, https://www.ncbi.nlm.nih.gov/bioproject/PRJNA476308/. LC-MS/MS raw data files are publically accessible under the MassIVE https://massive.ucsd.edu/https://massive.ucsd.edu/ accession no. MSV000082891.

## Competing interests

The authors declare that they have no competing interests.

## Funding

This work was supported from the China Scholarship Council and by Lundbeck Foundation grant R223-2016-179.

## Acknowledgements

We thank Ricardo R. da Silva for support in using the *in silico* annotation tool Network Annotation Propagation (NAP).

## References

Aksenov, A.A., Da Silva, R., Knight, R., Lopes, N.P., Dorrestein, P.C., 2017. Global chemical analysis of biology by mass spectrometry. Nat. Rev. Chem. https://doi.org/10.1038/s41570-017-0054.

Amar, J., Chabo, C., Waget, A., Klopp, P., Vachoux, C., Bermúdez-Humarán, L.G., Smirnova, N., Bergé, M., Sulpice, T., Lahtinen, S., Ouwehand, A., Langella, P., Rautonen, N., Sansonetti, P.J., Burcelin, R., 2011. Intestinal mucosal adherence and translocation of commensal bacteria at the early onset of type 2 diabetes: molecular mechanisms and probiotic treatment. EMBO Mol. Med. 3, 559–572. https://doi.org/10.1002/emmm.201100159.

Bäckhed, F., Ley, R.E., Sonnenburg, J.L., Peterson, D.A., Gordon, J.I., 2005. Host-bacterial mutualism in the human intestine. Science (80-. ). https://doi.org/10.1126/science.1104816.

Breton, J., Massart, S., Vandamme, P., De Brandt, E., Pot, B., Foligné, B., 2013. Ecotoxicology inside the gut: impact of heavy metals on the mouse microbiome. BMC Pharmacol. Toxicol. 14 (62). https://doi.org/10.1186/2050-6511-14-62.

Cani, P.D., Neyrinck, A.M., Fava, F., Knauf, C., Burcelin, R.G., Tuohy, K.M., Gibson, G.R., Delzenne, N.M., 2007. Selective increases of bifidobacteria in gut microflora improve high-fat-diet-induced diabetes in mice through a mechanism associated with endotoxaemia. Diabetologia 50, 2374–2383. https://doi.org/10.1007/s00125-007-0791-0.

Cani, P.D., Possemiers, S., Van De Wiele, T., Guiot, Y., Everard, A., Rottier, O., Geurts, L., Naslain, D., Neyrinck, A., Lambert, D.M., Muccioli, G.G., Delzenne, N.M., 2009. Changes in gut microbiota control inflammation in obese mice through a mechanism involving GLP-2-driven improvement of gut permeability. Gut 58, 1091–1103. https://doi.org/10.1136/gut.2008.165886.

Cascio, A., Stassi, G., Costa, G.B., Crisafulli, G., Rulli, I., Ruggeri, C., Iaria, C., 2005. Chryseobacterium indologenes bacteraemia in a diabetic child. J. Med. Microbiol. 54, 677–680. https://doi.org/10.1099/jmm.0.46036-0.

Chen, Y.W., Yang, C.Y., Huang, C.F., Hung, D.Z., Leung, Y.M., Liu, S.H., 2009. Heavy metals, islet function and diabetes development. Islets 1, 169–176. https://doi.org/10.4161/isl.1.3.9262.

Claus, S.P., Tsang, T.M., Wang, Y., Cloarec, O., Skordi, E., Martin, F.P., Rezzi, S., Ross, A., Kochhar, S., Holmes, E., Nicholson, J.K., 2008. Systemic multicompartmental effects of the gut microbiome on mouse metabolic phenotypes. Mol. Syst. Biol. 4. https://doi.org/10.1038/msb.2008.56.

Csardi, G., 2015. Package "igraph": network analysis and visualization author. In: R Packag. Version 1.0.1, pp. 1–462. https://doi.org/10.1177/001316446902900315.

da Silva, R.R., Wang, M., Nothias, L.F., van der Hooft, J.J.J., Caraballo-Rodríguez, A.M., Fox, E., Balunas, M.J., Klassen, J.L., Lopes, N.P., Dorrestein, P.C., 2018. Propagating annotations of molecular networks using in silico fragmentation. PLoS Comput. Biol. 14, 1–26. https://doi.org/10.1371/journal.pcbi.1006089.

Diawara, M.M., Litt, J.S., Unis, D., Alfonso, N., Martinez, L., Crock, J.G., Smith, D.B., Carsella, J., 2006. Arsenic, Cadmium, Lead, and Mercury in surface soils, Pueblo, Colorado: implications for population health risk. Environ. Geochem. Health 28, 297–315. https://doi.org/10.1007/s10653-005-9000-6.

Edgar, R.C., 2013. UPARSE: highly accurate OTU sequences from microbial amplicon reads. Nat. Methods 10, 996–998. https://doi.org/10.1038/nmeth.2604.

Edwards, J.R., Prozialeck, W.C., 2009. Cadmium, diabetes and chronic kidney disease. Toxicol. Appl. Pharmacol. 238, 289–293. https://doi.org/10.1016/j.taap.2009.03.007.

El Muayed, M., Raja, M.R., Zhang, X., MacRenaris, K.W., Bhatt, S., Chen, X., Urbanek, M., O'Halloran, T.V., Lowe, W.L., 2012. Accumulation of cadmium in insulin-producing β cells. Islets 4, 405–416. https://doi.org/10.4161/isl.23101.

Everard, A., Cani, P.D., 2013. Diabetes, obesity and gut microbiota. Best Pract. Res. Clin. Gastroenterol. 27, 73–83. https://doi.org/10.1016/j.bpg.2013.03.007.

Everard, A., Belzer, C., Geurts, L., Ouwerkerk, J.P., Druart, C., Bindels, L.B., Guiot, Y., 2013. Cross-talk between *Akkermansia muciniphila* and intestinal epithelium controls diet-induced obesity. Proc. Natl. Acad. Sci. U. S. A. 110, 9066–9071. https://doi.org/10.1073/pnas.1219451110/-/DCSupplemental.www.pnas.org/cgi/doi/10.1073/pnas.1219451110.

Fukushima, A., 2013. DiffCorr: an R package to analyze and visualize differential correlations in biological networks. Gene 518, 209–214. https://doi.org/10.1016/j.gene.2012.11.028.

Gao, Z., Yin, J., Zhang, J., Ward, R.E., Martin, R.J., Lefevre, M., Cefalu, W.T., Ye, J., 2010. Butyrate improves insulin sensitivity and increases energy expenditure in mice — Diab … page 1 of 14 butyrate improves insulin sensitivity and increases energy expenditure in mice butyrate improves insulin sensitivity and increases energy expenditure in. Diabetes 58, 1–14. https://doi.org/10.2337/db08-1637.

Guariguata, L., Whiting, D.R., Hambleton, I., Beagley, J., Linnenkamp, U., Shaw, J.E., 2014. Global estimates of diabetes prevalence for 2013 and projections for 2035. Diabetes Res. Clin. Pract. 103, 137–149. https://doi.org/10.1016/j.diabres.2013.11.002.

Guasch-Ferré, M., Hruby, A., Toledo, E., Clish, C.B., Martínez-González, M.A., Salas-Salvadó, J., Hu, F.B., 2016. Metabolomics in prediabetes and diabetes: a systematic review and meta-analysis. Diabetes Care. https://doi.org/10.2337/dc15-2251.

Hansen, C.H.F., Krych, L., Nielsen, D.S., Vogensen, F.K., Hansen, L.H., Sørensen, S.J., Buschard, K., Hansen, A.K., 2012. Early life treatment with vancomycin propagates Akkermansia muciniphila and reduces diabetes incidence in the NOD mouse. Diabetologia 55, 2285–2294. https://doi.org/10.1007/s00125-012-2564-7.

He, C., Shan, Y., Song, W., 2015. Targeting gut microbiota as a possible therapy for diabetes. Nutr. Res. https://doi.org/10.1016/j.nutres.2015.03.002.

Heinzmann, S.S., Schmitt-Kopplin, P., 2015. Deep metabotyping of the murine gastrointestinal tract for the visualization of digestion and microbial metabolism. J. Proteome Res. 14, 2267–2277. https://doi.org/10.1021/acs.jproteome.5b00034.

Hill, C., Guarner, F., Reid, G., Gibson, G.R., Merenstein, D.J., Pot, B., Morelli, L., Canani, R.B., Flint, H.J., Salminen, S., Calder, P.C., Sanders, M.E., 2014. Expert consensus document: the international scientific association for probiotics and prebiotics consensus statement on the scope and appropriate use of the term probiotic. Nat. Rev. Gastroenterol. Hepatol. 11, 506–514. https://doi.org/10.1038/nrgastro.2014.66.

Huang, M., Joseph, J.W., 2014. Assessment of the metabolic pathways associated with glucose-stimulated biphasic insulin secretion. Endocrinology 155, 1653–1666. https://doi.org/10.1210/en.2013-1805.

Hughes, M.F., Beck, B.D., Chen, Y., Lewis, A.S., Thomas, D.J., 2011. Arsenic exposure and toxicology: a historical perspective. Toxicol. Sci. 123, 305–332. https://doi.org/10.1093/toxsci/kfr184.

Jääskeläinen, T., Paananen, J., Lindström, J., Eriksson, J.G., Tuomilehto, J., Uusitupa, M., 2013. Genetic predisposition to obesity and lifestyle factors-the combined analyses of twenty-six known BMI-and fourteen known waist:hip ratio (WHR)-associated variants in the Finnish Diabetes Prevention Study. Br. J. Nutr. 110, 1856–1865. https://doi.org/10.1017/S0007114513001116.

Jeon, J.Y., Ha, K.H., Kim, D.J., 2015. New risk factors for obesity and diabetes: environmental chemicals. J. Diabetes Investig. 6, 109–111. https://doi.org/10.1111/jdi.12318.

Keil, D.E., Berger-Ritchie, J., McMillin, G.A., 2011. Testing for toxic elements: a focus on arsenic, cadmium, lead, and mercury. Lab. Med. 42, 735–742. https://doi.org/10.1309/LMYKGU05BEPE7IAW.

Kim, D.J., Lee, M.S., Kim, K.W., Lee, M.K., 2001. Insulin secretory dysfunction and insulin resistance in the pathogenesis of Korean type 2 diabetes mellitus. Metabolism. 50, 590–593. https://doi.org/10.1053/meta.2001.22558.

Klindworth, A., Pruesse, E., Schweer, T., Peplies, J., Quast, C., Horn, M., Glöckner, F.O., 2013. Evaluation of general 16S ribosomal RNA gene PCR primers for classical and next-generation sequencing-based diversity studies. Nucleic Acids Res. 41. https://doi.org/10.1093/nar/gks808.

Kolaczyk, E.D., Csárdi, G., Csardi, G., 2014. Statistical Analysis of Network Data with R, Use R! https://doi.org/10.1007/978-0-387-88146-1

Kuhn, M., 2008. Caret package. J. Stat. Softw. 28, 1–26.

Larsen, N., Vogensen, F.K., Van Den Berg, F.W.J., Nielsen, D.S., Andreasen, A.S., Pedersen, B.K., Al-Soud, W.A., Sørensen, S.J., Hansen, L.H., Jakobsen, M., 2010. Gut microbiota in human adults with type 2 diabetes differs from non-diabetic adults. PLoS One 5. https://doi.org/10.1371/journal.pone.0009085.

Lebovitz, H.E., Banerji, M.A., 2005. Point: visceral adiposity is causally related to insulin resistance. Diabetes Care. https://doi.org/10.2337/diacare.28.9.2322.

Lin, H., An, Y., Hao, F., Wang, Y., Tang, H., 2016. Correlations of fecal metabonomic and microbiomic changes induced by high-fat diet in the pre-obesity state. Sci. Rep. 6. https://doi.org/10.1038/srep21618.

Liu, Y., Li, Y., Liu, K., Shen, J., 2014. Exposing to cadmium stress cause profound toxic effect on microbiota of the mice intestinal tract. PLoS One 9, 1–9. https://doi.org/10.1371/journal.pone.0085323.

Lozupone, C., Knight, R., 2005. UniFrac: a new phylogenetic method for comparing microbial communities. Appl. Environ. Microbiol. 71, 8228–8235. https://doi.org/10.1128/AEM.71.12.8228-8235.2005.

Lu, K., Abo, R.P., Schlieper, K.A., Graffam, M.E., Levine, S., Wishnok, J.S., Swenberg, J.A., Tannenbaum, S.R., Fox, J.G., 2014. Arsenic exposure perturbs the gut microbiome and its metabolic profile in mice: an integrated metagenomics and metabolomics analysis. Environ. Health Perspect. 122, 284–291. https://doi.org/10.1289/ehp.1307429.

Lu, Y.Z., Ding, Z.W., Ding, J., Fu, L., Zeng, R.J., 2015. Design and evaluation of universal 16S rRNA gene primers for high-throughput sequencing to simultaneously detect DAMO microbes and anammox bacteria. Water Res. 87, 385–394.

Madeddu, R., Muresu, E., Montella, A., Chessa, G., Cherchi, G.B., Piras, P., Vargiu, P., Tolu, P., Pirino, A., Prados, J.C., Castiglia, P., 2009. Low cadmium concentration in whole blood from residents of Northern Sardinia (Italy) with special reference to smoking habits. J. Prev. Med. Hyg. 50, 46–52.

Magoč, T., Salzberg, S.L., 2011. FLASH: fast length adjustment of short reads to improve genome assemblies. Bioinformatics 27, 2957–2963. https://doi.org/10.1093/bioinformatics/btr507.

Mahendran, Y., Jonsson, A., Have, C.T., Allin, K.H., Witte, D.R., Jørgensen, M.E., Grarup, N., Pedersen, O., Kilpeläinen, T.O., Hansen, T., 2017. Genetic evidence of a causal effect of insulin resistance on branched-chain amino acid levels. Diabetologia 60, 873–878. https://doi.org/10.1007/s00125-017-4222-6.

McMurdie, P.J., Holmes, S., 2013. Phyloseq: an R package for reproducible interactive analysis and graphics of microbiome census data. PLoS One 8. https://doi.org/10.1371/journal.pone.0061217.

Miquel, S., Martin, R., Bridonneau, C., Robert, V., Sokol, H., Bermúdez-Humarán, L.G., Thomas, M., Langella, P., 2014. Ecology and metabolism of the beneficial intestinal commensal bacterium Faecalibacterium prausnitzii. Gut Microbes. https://doi.org/10.4161/gmic.27651.

National Research Council, 1999. Arsenic in Drinking Water. National Academies Press.

Nielsen, D.S., Møller, P.L., Rosenfeldt, V., Pærregaard, A., Michaelsen, F., Jakobsen, M., 2003. Case Study of the Distribution of Mucosa-Associated Bifidobacterium Species , Lactobacillus Species , and Other Lactic Acid Bacteria in the Human Colon Case Study of the Distribution of Mucosa-Associated Bifidobacterium Species , Lactobacillus Species , a. Appl. Environ. Microbiol. 69, 7545–7548. https://doi.org/10.1128/AEM.69.12.75451

Oksanen, J., Kindt, R., Legendre, P., O'Hara, B., Simpson, G.L., Solymos, P.M., Stevens, M.H.H., Wagner, H., 2008. The vegan package. Community Ecol. Packag. 190. https://doi.org/10.4135/9781412971874.n145.

Oksanen, J., Blanchet, F.G., Kindt, R., Legendre, P., Minchin, P.R., O'Hara, R.B., Simpson, G.L., Solymos, P., Henry, M., Stevens, H., Wagner, H., 2016. Vegan: community ecology package. R Packag. version 2.4-1. https//CRAN.R-project.org/package=vegan 280.

Pedersen, H.K., Gudmundsdottir, V., Nielsen, H.B., Hyotylainen, T., Nielsen, T., Jensen, B.A.H., Forslund, K., Hildebrand, F., Prifti, E., Falony, G., Le Chatelier, E., Levenez, F., Doré, J., Mattila, I., Plichta, D.R., Pöhö, P., Hellgren, L.I., Arumugam, M., Sunagawa, S., Vieira-Silva, S., Jørgensen, T., Holm, J.B., Trošt, K., Kristiansen, K., Brix, S., Raes, J., Wang, J., Hansen, T., Bork, P., Brunak, S., Oresic, M., Ehrlich, S.D., Pedersen, O., 2016. Human gut microbes impact host serum metabolome and insulin sensitivity. Nature 535, 376–381. https://doi.org/10.1038/nature18646.

Phipson, B., Smyth, G.K., 2010. Permutation P-values should never be zero: calculating exact P-values when permutations are randomly drawn. Stat. Appl. Genet. Mol. Biol. 9. https://doi.org/10.2202/1544-6115.1585.

Pichette, J., Fynn-Sackey, N., Gagnon, J., 2017. Hydrogen sulfide and sulfate prebiotic stimulates the secretion of GLP-1 and improves glycemia in male mice. Endocrinology 158, 3416–3425. https://doi.org/10.1210/en.2017-00391.

Plovier, H., Everard, A., Druart, C., Depommier, C., Van Hul, M., Geurts, L., Chilloux, J., Ottman, N., Duparc, T., Lichtenstein, L., Myridakis, A., Delzenne, N.M., Klievink, J., Bhattacharjee, A., Van Der Ark, K.C.H., Aalvink, S., Martinez, L.O., Dumas, M.E., Maiter, D., Loumaye, A., Hermans, M.P., Thissen, J.P., Belzer, C., De Vos, W.M., Cani, P.D., 2017. A purified membrane protein from Akkermansia muciniphila or the pasteurized bacterium improves metabolism in obese and diabetic mice. Nat. Med. 23, 107–113. https://doi.org/10.1038/nm.4236.

Pluskal, T., Castillo, S., Villar-Briones, A., Orešič, M., 2010. MZmine 2: modular framework for processing, visualizing, and analyzing mass spectrometry-based molecular profile data. BMC Bioinf. 11. https://doi.org/10.1186/1471-2105-11-395.

Qin, J., Li, Y., Cai, Z., Li, S., Zhu, J., Zhang, F., Liang, S., Zhang, W., Guan, Y., Shen, D., Peng, Y., Zhang, D., Jie, Z., Wu, W., Qin, Y., Xue, W., Li, J., Han, L., Lu, D., Wu, P., Dai, Y., Sun, X., Li, Z., Tang, A., Zhong, S., Li, X., Chen, W., Xu, R., Wang, M., Feng, Q., Gong, M., Yu, J., Zhang, Y., Zhang, M., Hansen, T., Sanchez, G., Raes, J., Falony, G., Okuda, S., Almeida, M., LeChatelier, E., Renault, P., Pons, N., Batto, J.-M., Zhang, Z., Chen, H., Yang, R., Zheng, W., Li, S., Yang, H., Wang, J., Ehrlich, S.D., Nielsen, R., Pedersen, O., Kristiansen, K., Wang, J., 2012. A metagenome-wide association study of gut microbiota in type 2 diabetes. Nature 490, 55–60. https://doi.org/10.1038/nature11450.

R Development Core Team, R, 2011. R: a language and environment for statistical computing. In: R Foundation for Statistical Computing, https://doi.org/10.1007/978-3-540-74686-7.

Roediger, W.E., 1980. Role of anaerobic bacteria in the metabolic welfare of the colonic mucosa in man. Gut 21, 793–798. https://doi.org/10.1136/gut.21.9.793.

Russell, W.M.S., Burch, R.L., 1959. Chapter 5–7, in: The Principles of Humane Experimental Technique.

Schlecht, I., Gronwald, W., Behrens, G., Baumeister, S.E., Hertel, J., Hochrein, J., Zacharias, H.U., Fischer, B., Oefner, P.J., Leitzmann, M.F., 2017. Visceral adipose tissue but not subcutaneous adipose tissue is associated with urine and serum metabolites. PLoS One 12. https://doi.org/10.1371/journal.pone.0175133.

Schloss, P.D., Westcott, S.L., Ryabin, T., Hall, J.R., Hartmann, M., Hollister, E.B., Lesniewski, R.A., Oakley, B.B., Parks, D.H., Robinson, C.J., Sahl, J.W., Stres, B., Thallinger, G.G., Van Horn, D.J., Weber, C.F., 2009. Introducing mothur: open-source, platform-independent, community-supported software for describing and comparing microbial communities. Appl. Environ. Microbiol. 75, 7537–7541. https://doi.org/10.1128/AEM.01541-09.

Suwazono, Y., Kido, T., Nakagawa, H., Nishijo, M., Honda, R., Kobayashi, E., Dochi, M., Nogawa, K., 2009. Biological half-life of cadmium in the urine of inhabitants after cessation of cadmium exposure. Biomarkers 14, 77–81. https://doi.org/10.1080/13547500902730698.

Vrieze, A., Out, C., Fuentes, S., Jonker, L., Reuling, I., Kootte, R.S., Van Nood, E., Holleman, F., Knaapen, M., Romijn, J.A., Soeters, M.R., Blaak, E.E., Dallinga-Thie, G.M., Reijnders, D., Ackermans, M.T., Serlie, M.J., Knop, F.K., Holst, J.J., Van Der Ley, C., Kema, I.P., Zoetendal, E.G., De Vos, W.M., Hoekstra, J.B.L., Stroes, E.S., Groen, A.K., Nieuwdorp, M., 2014. Impact of oral vancomycin on gut microbiota, bile acid metabolism, and insulin sensitivity. J. Hepatol. 60, 824–831. https://doi.org/10.1016/j.jhep.2013.11.034.

Walker, A., Lucio, M., Pfitzner, B., Scheerer, M.F., Neschen, S., De Angelis, M.H., Hartmann, A., Schmitt-Kopplin, P., 2014. Importance of sulfur-containing metabolites in discriminating fecal extracts between normal and Type-2 diabetic mice. J. Proteome Res. 13, 4220–4231. https://doi.org/10.1021/pr500046b.

Wang, M., Carver, J.J., Phelan, V.V., Sanchez, L.M., Garg, N., Peng, Y., Nguyen, D.D., Watrous, J., Kapono, C.A., Luzzatto-Knaan, T., Porto, C., Bouslimani, A., Melnik, A.V., Meehan, M.J., Liu, W.T., Crüsemann, M., Boudreau, P.D., Esquenazi, E., Sandoval-Calderón, M., Kersten, R.D., Pace, L.A., Quinn, R.A., Duncan, K.R., Hsu, C.C., Floros, D.J., Gavilan, R.G., Kleigrewe, K., Northen, T., Dutton, R.J., Parrot, D., Carlson, E.E., Aigle, B., Michelsen, C.F., Jelsbak, L., Sohlenkamp, C., Pevzner, P., Edlund, A., McLean, J., Piel, J., Murphy, B.T., Gerwick, L., Liaw, C.C., Yang, Y.L., Humpf, H.U., Maansson, M., Keyzers, R.A., Sims, A.C., Johnson, A.R., Sidebottom, A.M., Sedio, B.E., Klitgaard, A., Larson, C.B., Boya, C.A.P., Torres-Mendoza, D., Gonzalez, D.J., Silva, D.B., Marques, L.M., Demarque, D.P., Pociute, E., O'Neill, E.C., Briand, E., Helfrich, E.J.N., Granatosky, E.A., Glukhov, E., Ryffel, F., Houson, H., Mohimani, H., Kharbush, J.J., Zeng, Y., Vorholt, J.A., Kurita, K.L., Charusanti, P., McPhail, K.L., Nielsen, K.F., Vuong, L., Elfeki, M., Traxler, M.F., Engene, N., Koyama, N., Vining, O.B., Baric, R., Silva, R.R., Mascuch, S.J., Tomasi, S., Jenkins, S., Macherla, V., Hoffman, T., Agarwal, V., Williams, P.G., Dai, J., Neupane, R., Gurr, J., Rodríguez, A.M.C., Lamsa, A., Zhang, C., Dorrestein, K., Duggan, B.M., Almaliti, J., Allard, P.M., Phapale, P., Nothias, L.F., Alexandrov, T., Litaudon, M., Wolfender, J.L., Kyle, J.E., Metz, T.O., Peryea, T., Nguyen, D.T., VanLeer, D., Shinn, P., Jadhav, A., Müller, R., Waters, K.M., Shi, W., Liu, X., Zhang, L., Knight, R., Jensen, P.R., Palsson, B., Pogliano, K., Linington, R.G., Gutiérrez, M., Lopes, N.P., Gerwick, W.H., Moore, B.S., Dorrestein, P.C., Bandeira, N., 2016. Sharing and community curation of mass spectrometry data with Global Natural Products Social Molecular Networking. Nat. Biotechnol. https://doi.org/10.1038/nbt.3597.

Watrous, J., Roach, P., Alexandrov, T., Heath, B.S., Yang, J.Y., Kersten, R.D., van der Voort, M., Pogliano, K., Gross, H., Raaijmakers, J.M., Moore, B.S., Laskin, J., Bandeira, N., Dorrestein, P.C., 2012. Mass spectral molecular networking of living microbial colonies. Proc. Natl. Acad. Sci. 109, E1743–E1752. https://doi.org/10.1073/pnas.1203689109.

Wild, Sarah, Roglic, Gojka, Green, Anders, Sicree, Richard, Hilary, K., 2004. Global prevalence of diabetes: estimates for the year 2000 and projection for 2030. Diabetes Care 27, 1047–1053. https://doi.org/10.2337/diacare.27.5.1047.

Wu, X., Ma, C., Han, L., Nawaz, M., Gao, F., Zhang, X., Yu, P., Zhao, C., Li, L., Zhou, A., Wang, J., Moore, J.E., Millar, B.C., Xu, J., 2010. Molecular characterisation of the faecal microbiota in patients with type II diabetes. Curr Microbiol 61, 69–78. https://doi.org/10.1007/s00284-010-9582-9.

Xu, J., Lian, F., Zhao, L., Zhao, Y., Chen, X., Zhang, X., Guo, Y., Zhang, C., Zhou, Q., Xue, Z., Pang, X., Zhao, L., Tong, X., 2015. Structural modulation of gut microbiota during alleviation of type 2 diabetes with a Chinese herbal formula. ISME J. 9, 552–562. https://doi.org/10.1038/ismej.2014.177.

Yang, Y., Zheng, L., Wang, L., Wang, S., Wang, Y., Han, Z., 2015. Effects of high fructose and salt feeding on systematic metabonome probed via1H NMR spectroscopy. Magn. Reson. Chem. 53, 295–303. https://doi.org/10.1002/mrc.4198.

Yu, L., Zhao, X.K., Cheng, M.L., Yang, G.Z., Wang, B., Liu, H.J., Hu, Y.X., Zhu, L.L., Zhang, S., Xiao, Z.W., Liu, Y.M., Zhang, B.F., Mu, M., 2017. Saccharomyces boulardii administration changes gut microbiota and attenuates D-galactosamine-induced liver injury. Sci. Rep. 7. https://doi.org/10.1038/s41598-017-01271-9.

Zarling, E.J., Ruchim, M.A., 1987. Protein origin of the volatile fatty-acids isobutyrate and isovalerate in human stool. J. Lab. Clin. Med. 109, 566–670.

Zarrinpar, A., Chaix, A., Xu, Z.Z., Chang, M.W., Marotz, C.A., Saghatelian, A., Knight, R., Panda, S., 2018. Antibiotic-induced microbiome depletion alters metabolic homeostasis by affecting gut signaling and colonic metabolism. Nat. Commun. 9. https://doi.org/10.1038/s41467-018-05336-9.

Zhang, S., Jin, Y., Zeng, Z., Liu, Z., Fu, Z., 2015. Subchronic exposure of mice to cadmium perturbs their hepatic energy metabolism and gut microbiome. Chem. Res. Toxicol. 28, 2000–2009. https://doi.org/10.1021/acs.chemrestox.5b00237.

Zhang, Q., Wu, Y., Wang, J., Wu, G., Long, W., Xue, Z., Wang, L., Zhang, X., Pang, X., Zhao, Y., Zhao, L., Zhang, C., 2016. Accelerated dysbiosis of gut microbiota during aggravation of DSS-induced colitis by a butyrate-producing bacterium. Sci. Rep. 6. https://doi.org/10.1038/srep27572.